$MgAl_2O_4:Mn^{2+}$ Red-Emitting Phosphor: Influence of MgF_2 Flux on the Microstructure and Luminescence Properties

Shan Li[a,#] , Shu-Yu Zhao[a,#], Tian-Nan Ye[c], Xue-Yan Wu[b], Kai-Xue Wang[a], Xiao Wei[a,*] and Jie-Sheng Chen[a]

[a]*School of Chemistry and Chemical Engineering, Hirano Institute for Materials Innovation, Shanghai Jiao Tong University Dongchuan Road No.800, Shanghai, 200240, P. R. China*

[b]*School of Materials Science and Engineering, Hirano Institute for Materials Innovation, Shanghai Jiao Tong University Dongchuan Road No.800, Shanghai, 200240, P. R. China*

[c]*Materials Research Center for Element Strategy, Tokyo Institute of Technology, 4259 Nagatsuta-cho, Midori-ku, Yokohama, Kanagawa 226-8503, Japan*

Abstract: A serial of Mn ions doped $MgAl_2O_4$ phosphors, exhibiting only red light centred at 650 nm, have been prepared by a solid state reaction (SSR) with and without MgF_2 flux. These phosphors have been characterized by X-ray diffraction (XRD), scanning electron microscopy (SEM), and electron paramagnetic resonance (EPR) measurements. EPR result demonstrates that Mn ions exist as +2 valence. The emission intensity of the phosphors varies with Mn^{2+} concentration. The addition of MgF_2 flux to the reactants enhances the luminescence properties through elevating the crystallinity, regulating the morphology and particle size of the $MgAl_2O_4:Mn^{2+}$ phosphor. The phosphor $MgAl_2O_4$:0.10%Mn^{2+} with 12 wt% MgF_2 flux shows the best emission performance.

Keywords: Magnesium aluminate, Manganese doping, Red phosphor, Solid state reaction, MgF_2 Flux.

INTRODUCTION

As a new solid-state light source, light emitting diodes (LEDs) have received much attention due to their advantages of long lifetime, energy savings, small volume, reliability, and environmental-friendliness over traditional incandescent and fluorescent lamps [1-6]. However, LEDs with multiple emission wavelength chips have deteriorating color temperature and luminous efficiency due to the different lifetimes and stabilities of the chips [7]. It is well-known that the commercially available white LEDs are currently manufactured by combining a blue InGaN chip with a yellow-emitting phosphor (YAG:Ce^{3+}) [8]. Although the conversion efficiency is high, the color deficiency in the red region makes this white LEDs exhibit poor color rendering index (CRI) [9-11]. Therefore, in order to improve the CRI, it is important to develop new red emitting phosphors which can be excited under near-UV or blue region.

In recent years, rare-earth (RE) ions, particularly Eu^{3+}, have become good candidates for luminescent centers in red emitting phosphors. However, the limited reserve and restricted supply of RE elements lead to the high cost of RE compounds. Thus the development of new red phosphors with non-RE elements has received considerable attention. Manganese, an element with multiple oxidation states, has been considered as a promising alternative of RE elements for the preparation of phosphors. The valence and location of Mn ions in the host lattices determine the luminescence properties of Mn doped phosphors. For example, Mn^{4+} activated A_2SiF_6, A_2GeF_6 (A = Na, K), B_2SnF_6 (B = Na, Cs), $CaAl_{12}O_{19}$ and $3.5MgO{\cdot}0.5MgF_2{\cdot}GeO_2$ exhibit red emission under the UV or blue light excitation, which is associated with the transition $^2E \rightarrow {}^4A_2$ of Mn^{4+} [12-19]. And in our recent work, $Mg_2TiO_4:Mn^{4+}$ prepared by the sol-gel method shows an efficient red light emission [20]. Mn^{2+} can also act as an activator in phosphors. For example, Mn^{2+} doped Zn_2SiO_4 emits green light, owing to the transition occurring between the $^4T_1$ and $^6A_1$ levels of Mn^{2+} [21]. Another typical example of the phosphors containing Mn^{2+} is $MgAl_2O_4:Mn^{2+}$. $MgAl_2O_4$ belongs to the cubic space group *Fd-3m* with a spinel crystal structure. Mn^{2+} with $3d^5$ electronic structure coordinates with four oxygen atoms to form [MnO_4] tetrahedral, similar to that of Mg^{2+} in $MgAl_2O_4$. The ionic radius of Mn^{2+} (0.67 Å) is close to that of Mg^{2+} (0.72 Å). Furthermore, they have the same valence state of +2. Therefore, the substitution of Mn^{2+} for Mg^{2+} in $MgAl_2O_4$ is highly feasible. Tomita *et al.* have reported $MgAl_2O_4:Mn^{2+}$ which generates two independent luminescence channels (green emission centered at 520 nm and red emission centred at 650 nm under UV

*Address correspondence to this author at the School of Chemistry and Chemical Engineering, Hirano Institute for Materials Innovation, Shanghai Jiao Tong University Dongchuan Road No.800, Shanghai, 200240, P. R. China; Fax: +86-21-54741297; E-mail: weixiao@sjtu.edu.cn

#These authors contribute to this work equally.

E-ISSN: 2311-8717/17

and blue irradiation respectively) [22]. As to the best of our knowledge, there is no report so far on a single red luminescence channel for phosphors containing Mn^{2+}, especially for $MgAl_2O_4:Mn^{2+}$ spinel under both UV and blue irradiation. This means that it must be under a light source with particular wavelength in order to get a single red emission applied in LEDs.

Among many preparation methods for phosphors, the solid-state reaction (SSR) method is still one of the most common and promising methods for the phosphor preparation in both laboratories and industries [23-24]. However, besides high reaction temperature, long time for pestle samples is necessary in SSR. Even so, the high chemical uniformity is not guaranteed [25-29]. In order to overcome the drawbacks of the conventional SSR method, flux has been introduced to the reaction system to accelerate the reaction kinetics by enhancing diffusion coefficients. Kottaisamy *et al.* and Lee *et al.* confirmed that the addition of flux can obviously affect the growth conditions and the products generated [30-31]. It has been shown that the addition of fluxes such as MgF_2, BaF_2 NaF, H_3BO_3 and H_3BO_3/BaF_2 positively affects the crystallite size distribution, crystallinity and emission intensity of the phosphors [32-33]. However, there is no report on the preparation of $MgAl_2O_4:Mn^{2+}$ with enhanced luminescence properties by addition of any flux through a SSR route.

Herein, $MgAl_2O_4:Mn^{2+}$ phosphors with a single red luminescence channel have been prepared through solid state reaction with and without MgF_2 flux. The structure, morphology and crystallinity of products are characterized by XRD, SEM, and EPR techniques. The influence of flux on the microstructure and luminescence properties of the phosphors has also been investigated and elucidated.

MATERIALS AND METHODS

Materials and Preparation

A traditional solid state reaction method was used to prepare $MgAl_2O_4:Mn^{2+}$, with molar ratio $n_{Mn}/(n_{Mn}+n_{Mg})$ = 0%, 0.05%, 0.10%, 0.20% and 0.50%. Commercially available high-purity reagents (99.9 ~ 99.999%) of MgO, Al_2O_3, MnO and MgF_2 were used as raw materials. The adding weight ratio of MgF_2 flux varied from 0 wt% ~ 18 wt% to improve the luminescence properties. All the reagents were stoichiometrically mixed in an agate mortar and ball milled with zirconia balls for 2 h. Then the powders were calcined in a tube furnace at 900 ~ 1350 °C for 8 h with flowing oxygen. After gradually cooling to room temperature, the samples were then ground into fine powders.

Characterization

The powder X-ray diffraction (XRD) patterns were recorded on a Rigaku D/Max 2550 X-ray diffractometer with Cu Kα radiation (λ = 1.5418 Å, tube current and tube voltage are 30 mA and 40 kV respectively). The electron paramagnetic resonance (EPR) spectra were obtained on a JES-FA 200 electron paramagnetic resonance spectrometer (scanning frequency, 9.45 GHz; central field, 3360 G; scanning width, 8000 G; scanning power, 0.998 mW; scanning temperature, 25 °C). The scanning electron microscope (SEM) images were taken on a JEOL JSM-6700F field emission scanning electron microscope. The UV–vis absorption spectra were recorded on a Shimadzu UV-2450 spectrometer. The photoluminescence (PL) and photoluminescence excitation (PLE) spectra were recorded on a QM-4-CW (Photo technology international, Int. USA/CAN).

RESULTS AND DISCUSSION

Preparation of Mn^{2+} Doped Magnesium Aluminate

In SSR process, the temperature is a very important parameter, so the influence of calcination temperature on the crystal structure of $MgAl_2O_4$ has been investigated and discussed. Figure **1A** shows the XRD patterns of $MgAl_2O_4$ which were calcined at 900, 1100 and 1350 °C for 8 h respectively. The peaks located in the range between 10° and 80° correspond to (111), (220), (311), (222), (400), (422), (511), (440), (531), (620), (533) reflections of the cubic $MgAl_2O_4$ with a *Fd-3m* space group, consistent with that of JCPDS No. 75-1797. Small peaks are detected in the XRD patterns of the samples calcined at 900 and 1100 °C, attributed to the presence of MgO impurity (JCPDS No. 87-653). But after calcination at 1350 °C, a pure $MgAl_2O_4$ phase without the MgO impurity is obtained (c pattern in Figure **1A**). It is also noted that the intensity of the diffractions increases with the calcination temperature, indicating the better crystallinity. The XRD analyses revealed the appropriate temperature to generate pure-phased $MgAl_2O_4$ with high crystallinity is 1350 °C. Therefore, the temperature of 1350 °C is choosed for the preparation of Mn doped spinel $MgAl_2O_4$. Figure **1B** shows the XRD patterns of $MgAl_2O_4:Mn^{2+}$ samples with $n_{Mn}/(n_{Mn}+n_{Mg})$ molar ratio ranging from 0% to 0.50% prepared at 1350 °C. All of the diffractions of the as-obtained samples can be attributed to cubic $MgAl_2O_4$ without any impurity and the intensity of the diffractions indicates the high crystallinity of the samples prepared, suggesting that the incorporation of Mn ions does not lead to the variation of $MgAl_2O_4$ crystal structure. The

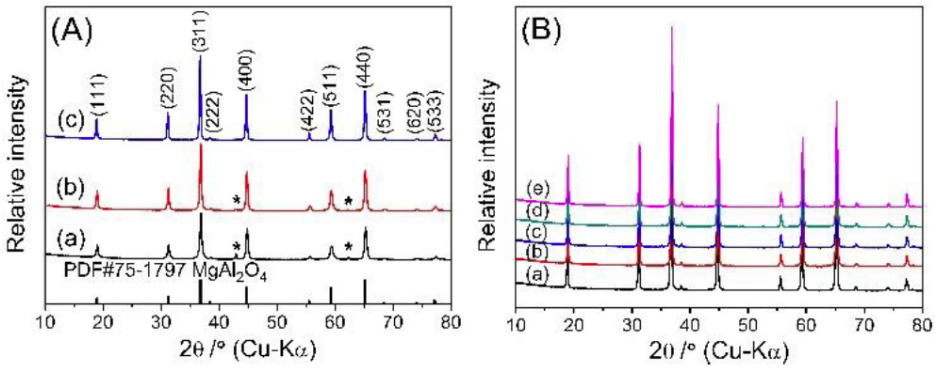

Figure 1: XRD patterns of samples (**A**) $MgAl_2O_4$ at different calcination temperatures: (a) 900 °C, (b) 1100 °C, (c) 1350 °C; (**B**) Mn-doped $MgAl_2O_4$ with $n_{Mn}/(n_{Mn}+n_{Mg})$: (a) 0%, (b) 0.05%, (c) 0.10%, (d) 0.20%, (e) 0.50%. Stars in (A) mark the impure phases of MgO.

lattice parameters of $MgAl_2O_4$ doped with various Mn^{2+} contents have been refined by the Win-CSD program [34]. As seen in Table 1, the lattice parameters decrease with the increase of Mn^{2+} content, which is attributed to the substitution of the smaller size Mn^{2+} (0.67 Å). Given the ionic sizes and taking into account of charge compensation, it is very likely that the Mn^{2+} ions substitute for the tetrahedrally coordinated Mg^{2+} in the $MgAl_2O_4$ host lattice.

In order to confirm the valence state of Mn ions in $MgAl_2O_4$, the EPR spectra of the samples are recorded in the low-field microwave response at room temperature. Figure **2** compares the EPR signals of the undoped $MgAl_2O_4$ and a representative of Mn-doped $MgAl_2O_4$ [$n_{Mn}/(n_{Mn}+n_{Mg})$ = 0.10%]. For pure $MgAl_2O_4$, there is no obvious EPR signals. But for Mn-doped $MgAl_2O_4$, the EPR spectrum shows a six-line hyperfine structure between 300 MT and 400 MT, which can be attributed to the interaction of unpaired electron with the Mn^{2+} nucleus (nucleus spin I = 5/2). It indicates that the doped Mn existed as ions with +2 valence in $MgAl_2O_4$.

Table 1: Lattice Parameters of the Samples with Various Mn Concentrations

Sample	$n_{Mn}/(n_{Mn}+n_{Mg})$	lattice parameter (Å)
a	0%	8.0920(2)
b	0.05%	8.0841(1)
c	0.10%	8.0833(3)
d	0.20%	8.0824(2)
e	0.50%	8.0809(1)

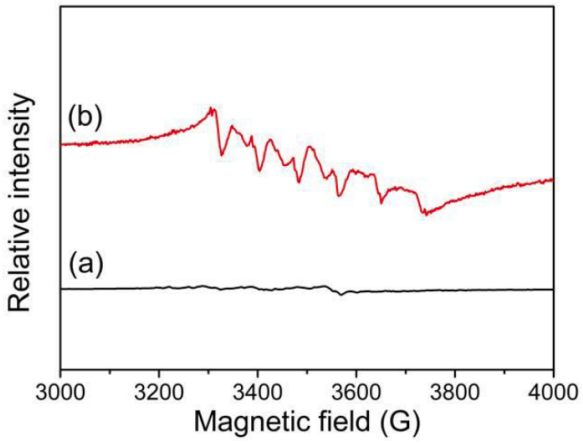

Figure 2: EPR spectra of the samples (a) $MgAl_2O_4$, (b) $MgAl_2O_4:Mn^{2+}$ with $n_{Mn}/(n_{Mn}+n_{Mg})$ = 0.10%.

Optical Properties of Mn^{2+} Doped Magnesium Aluminate

The substitution of Mn^{2+} for Mg-sites has an obvious effect on the UV-vis absorption behavior of the $MgAl_2O_4$ material. As shown in the UV-vis absorption spectra (Figure **3**), the absorption of $MgAl_2O_4$ is mainly located in the ultraviolet region (wavelength below 350 nm). A new absorption band within 400 and 600 nm appears for the Mn doped samples. The response

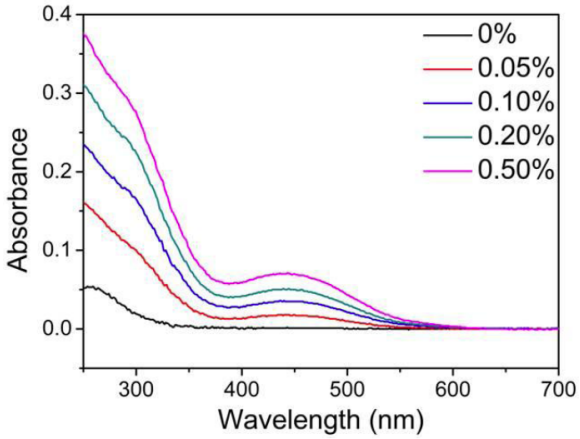

Figure 3: The room-temperature UV-vis absorption spectra of $MgAl_2O_4:Mn^{2+}$ with $n_{Mn}/(n_{Mn}+n_{Mg})$: 0%, 0.05%, 0.10%, 0.20% and 0.50%.

intensity of this band significant increases with the content of Mn^{2+} doped. The presence of the new absorption band indicates that new energy levels in the forbidden band of the host $MgAl_2O_4$ are formed due to the Mn doping, consistent with the observation in Mn^{2+} doped ZnO [35].

Figure **4** shows the photoluminescence (PL) excitation and emission spectra of $MgAl_2O_4:Mn^{2+}$ with $n_{Mn}/(n_{Mn}+n_{Mg})$ of 0%, 0.05%, 0.10%, 0.20% and 0.50%. Red emission intensity variation of the Mn-doped samples can be clearly observed from the photographs taken with a digital camera under UV light irradiation (Figure **4a**). Emission spectra of the samples under 435 nm excitation are shown in Figure **4b**. The samples doped with Mn ions exhibit only red emission centred at 650 nm. The intensity of the red emission depends on the amount of Mn^{2+} doped into the $MgAl_2O_4$ host. As shown in Figure **4c**, the emission intensity reaches the maximum when the Mn^{2+} doping concentration is 0.10%, and it then decreases with the concentration increasing from 0.10% to 0.50%. This phenomenon is attributed to the well-known concentration quenching effect [36]. Mn^{2+} ion pairs contributing to the concentration quenching effect is expected to be generated due to the reduced inter-ionic (Mn^{2+}-Mn^{2+}) distance resulting from the high doping concentration in the host lattice. The maximum emission of the samples is located at 650 nm, which can be assigned to the charge-transfer deexcitation associated with Mn^{2+} ion. The red emission process corresponds to a finite density of Mg^{2+} deficiencies existing in the spinel $MgAl_2O_4$. Due to the compensation of Mg^{2+} deficiency by Mn^{2+} doping, the luminescence quality is improved, coinciding with the assignment of Mn^{2+} ion to T_d *(A)* site. When the electron–hole pair is optically created, Mn^{2+} in *A* site will attract a hole at first, resulting in the formation of Mn^{3+} ($3d^4$), an intermediate state. Then an electron in the conduction band is radiatively annihilated, leading to the formation of the electronic ground state of Mn^{2+} ($3d^5$). On the other hand, it is also possible for the electron in the conduction band trapped by Mn^{2+} ion at first, generating an intermediate state. Then the hole radiatively annihilates in the valence band, generating the electronic ground state of Mn^{2+} ($3d^5$). It is possible that the luminescence phenomenon will take place both in the electron and hole trapping processes, in good agreement with those reported by Tomita *et al.* and Singh *et al*. [22, 37]. Figure **4d** shows the excitation spectrum of $MgAl_2O_4:Mn^{2+}$ with $n_{Mn}/(n_{Mn}+n_{Mg})$ = 0.10%. The excitation peaks are mainly located at 290 nm and 435 nm. The excitation band at 290 nm is induced

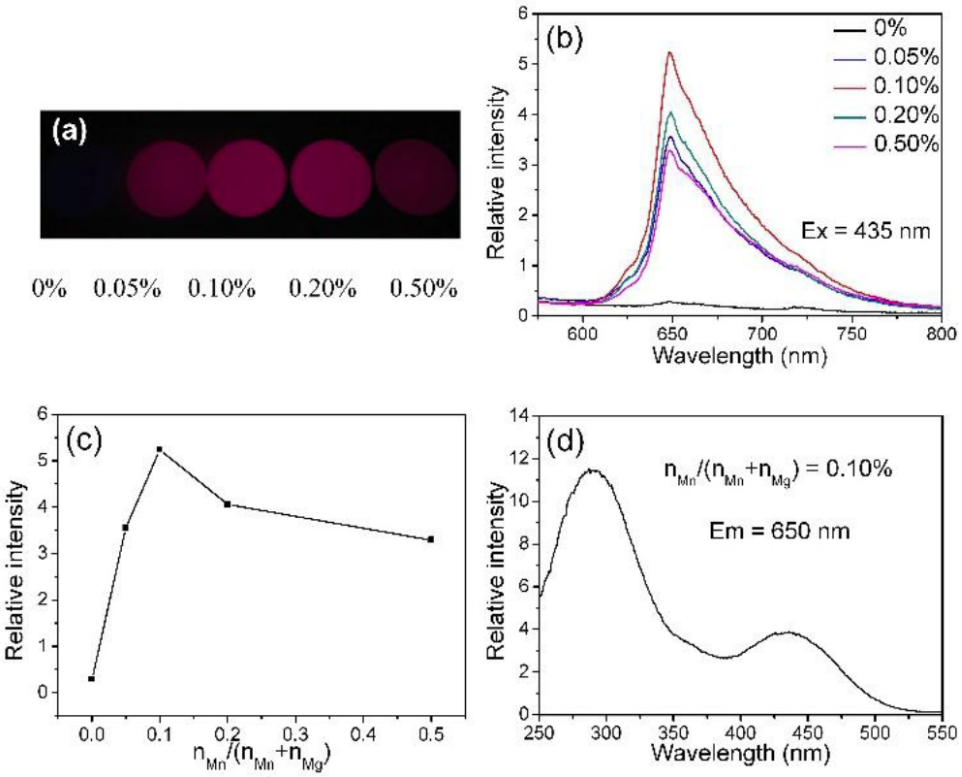

Figure 4: (**a**) Optical photos, (**b**) emission spectra, (**c**) concentration dependence of the relative emission intensity of $MgAl_2O_4:Mn^{2+}$ samples. $n_{Mn}/(n_{Mn}+n_{Mg})$: 0%, 0.05%, 0.10%, 0.20%, 0.50% respectively, and (**d**) excitation spectrum of $MgAl_2O_4:Mn^{2+}$, $n_{Mn}/(n_{Mn}+n_{Mg})$ = 0.10%.

mainly by the optical absorption which excites an electron–hole pair, similarly to those reported by Han *et al*. [38]. Whereas the broad excitation band at 435 nm is partially induced by the d-d transition $^6A_1 \rightarrow {}^4T_2$ of Mn^{2+}. It is noted that similar emission spectra with that shown in Figure **4b** are also received when the samples are excited under 290 nm.

Effect of MgF_2 Flux on Mn-Doped Magnesium Aluminate

In order to improve the luminescence properties of the Mn doped $MgAl_2O_4$ phosphor, MgF_2 flux is introduced to the reaction system. The $n_{Mn}/(n_{Mn}+n_{Mg})$ molar ratio of Mn^{2+} doped in the host is fixed to 0.10% to investigate the influence of the flux on the luminescence properties of the phosphors. The red emission intensity variation of the samples prepared with different weight ratios of MgF_2 can be observed from the digital photographs (Figure **5a**). The emission spectra of $MgAl_2O_4$:0.10%Mn^{2+} with different weight ratios of MgF_2 flux under 435 nm excitation are shown in Figure **5b**. Obviously, the emission intensity of $MgAl_2O_4$:0.10%Mn^{2+} with MgF_2 flux is higher than that of the sample without MgF_2. It is also observed that the red emission intensity gradually enhances and then decreases with the weight ratio of MgF_2, with the maximum emission intensity at MgF_2 weight ratio of 12 wt%. This is because the constituent ions of flux remain in the host lattice as defects that degrade the intensity [39]. Figure **5d** shows the excitation spectrum of $MgAl_2O_4$:0.10%Mn^{2+} with 12 wt% MgF_2 flux. The excitation peaks are mainly located at 290 nm and 435 nm, consistent with those of $MgAl_2O_4:Mn^{2+}$ phosphors prepared without MgF_2, suggesting that the addition of flux does not change the emission and excitation positions of $MgAl_2O_4:Mn^{2+}$ phosphors.

The luminescence properties are closely related to the crystallinity, particle size, and morphology of the Mn-doped $MgAl_2O_4$ phosphors prepared with the presence of MgF_2 flux. High crystallinity and relatively large particle size may suppress the amount of defects in the crystal structures, which leads to the improvement of emission intensity of the samples. The XRD patterns of $MgAl_2O_4$:0.10%Mn^{2+} prepared with various MgF_2 weight ratios are shown in Figure **6**. The strong diffractions of the samples are attributed to the cubic $MgAl_2O_4$. It can be seen that no distinctive peaks corresponding to MgF_2 phase were observed, indicating the most of the MgF_2 flux was removed after powder calcination. However, further increasing MgF_2 weight ratio to the reaction system, small amount of MgO impurity present in the final products, derived from the decomposition and oxidation of MgF_2 at high temperature in oxygen atmosphere (peaks marked with star in Figure **6**). The diffraction intensity of the samples with MgF_2 are higher than that of the sample

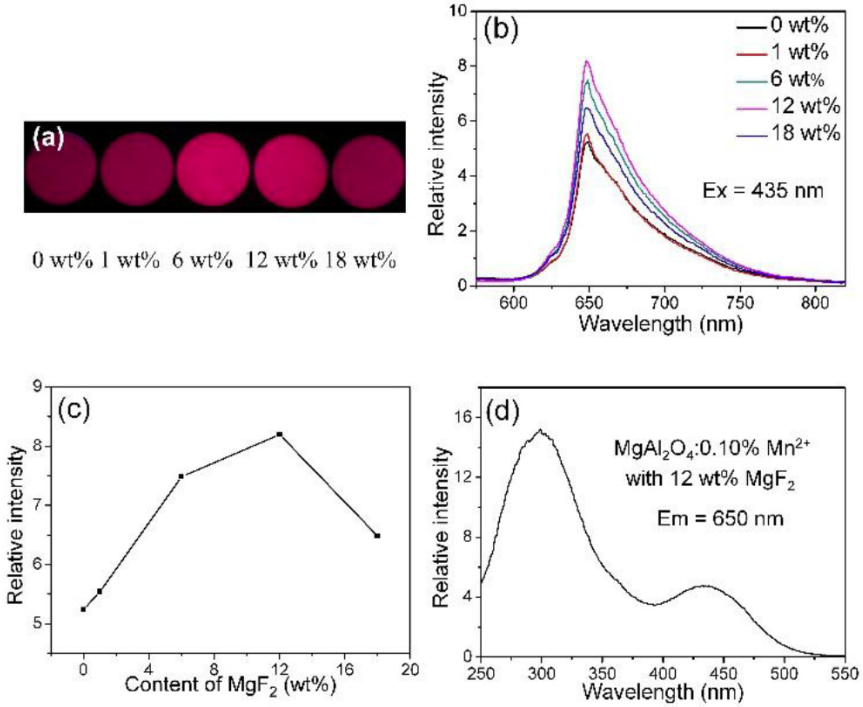

Figure 5: (**a**) Optical photos, (**b**) emission spectra, (**c**) relative emission intensity of $MgAl_2O_4$:0.10%Mn^{2+} with different weight ratios of MgF_2 flux (0 wt%, 1 wt%, 6 wt%, 12 wt%, 18 wt%), and (**d**) excitation spectrum of $MgAl_2O_4$:0.10%Mn^{2+} with 12 wt% MgF_2 flux.

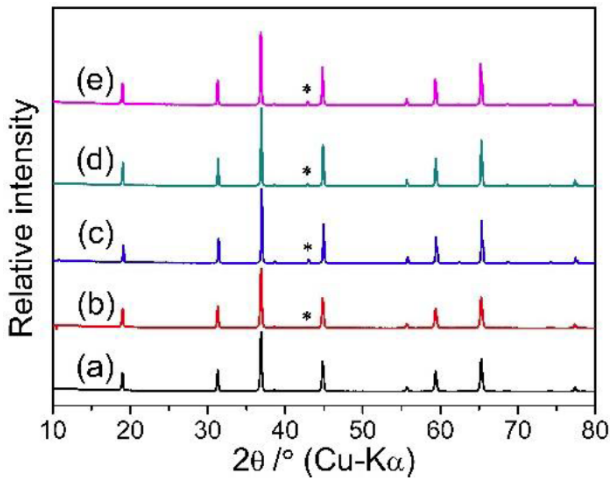

Figure 6: XRD patterns $MgAl_2O_4$:0.10%Mn^{2+} with different weight ratios of MgF_2 flux. (a) 0 wt%, (b) 1 wt%, (c) 6 wt%, (d) 12 wt%, (e) 18 wt%. Stars in (a) mark the impure phases of MgO.

without MgF_2, indicating the crystallinity of the phosphor is increased. The maximum intensities for diffraction peaks occurred when the MgF_2 flux weight ratio is 12 wt%. When the MgF_2 weight ratio is increased further, the intensity of the diffraction peaks decreases. Figure **7** shows the SEM images of $MgAl_2O_4$:0.10%Mn^{2+} with different weight ratios of MgF_2 flux (0 wt% ~ 18 wt%). It is observed that the particle size of the phosphors increases with MgF_2 weight ratio. Molten flux may facilitate the slide and rotation of particles, providing opportunities for particle-particle contact and promoting the particle growth [40-41]. Thus the increase of MgF_2 weight ratio leads to the formation of larger and more regular particles with the higher crystallinity, significantly reducing the amount of defects on the surface and in the crystal structure of the phosphors. Based on the XRD analyses and the SEM observation, the crystallinity, particle size, and morphology of the Mn-doped $MgAl_2O_4$ phosphors can be well controlled by the addition of MgF_2 flux to reaction system. It is known that the regular morphology and optimal particle size can improve the packing density of phosphor materials and produce uniform luminescence centers [42]. The uniform distribution of the luminescent centers in samples $MgAl_2O_4$:0.10%Mn^{2+} with 0 wt% and 12 wt% MgF_2 flux is illustrated in Scheme **1**. There is a increscent inter-ionic (Mn^{2+}-Mn^{2+}) distance alleviating the concentration quenching effect and thus enhancing the emission intensity. As a result, the emission performance of the sample with MgF_2 flux is markedly superior to that of the sample without flux.

The variation in the packing density and the interaction of inter-ionic Mn^{2+}-Mn^{2+} are reflected on the EPR signal. Figure **8** shows the EPR spectra of the Mn-doped $MgAl_2O_4$ phosphors prepared with and without MgF_2 flux. It is obvious that the EPR signal of $MgAl_2O_4$:0.10%Mn^{2+} prepared with 12 wt% MgF_2 flux is more distinctive than that of the sample prepared without MgF_2, consistent with their luminescent performance results. The EPR signal of $MgAl_2O_4$:0.10%Mn^{2+} with 12 wt% MgF_2 flux is intensified compared to that of the sample without MgF_2, indicating that the regular morphology and appropriate particle size can improve the packing density and weaken the inter-ionic Mn^{2+}-Mn^{2+} interaction.

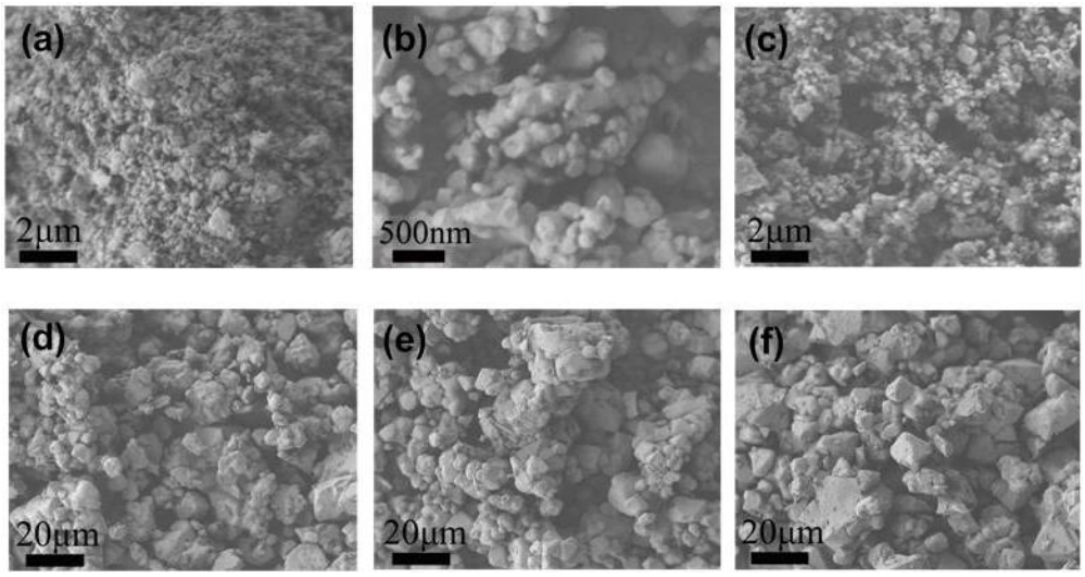

Figure 7: SEM images of $MgAl_2O_4$:0.10%Mn^{2+} with weight ratios of MgF_2 flux: (**a-b**) different magnification factors for samples with 0 wt%, (**c**) 1 wt%, (**d**) 6 wt%, (**e**) 12 wt%, (**f**) 18 wt%.

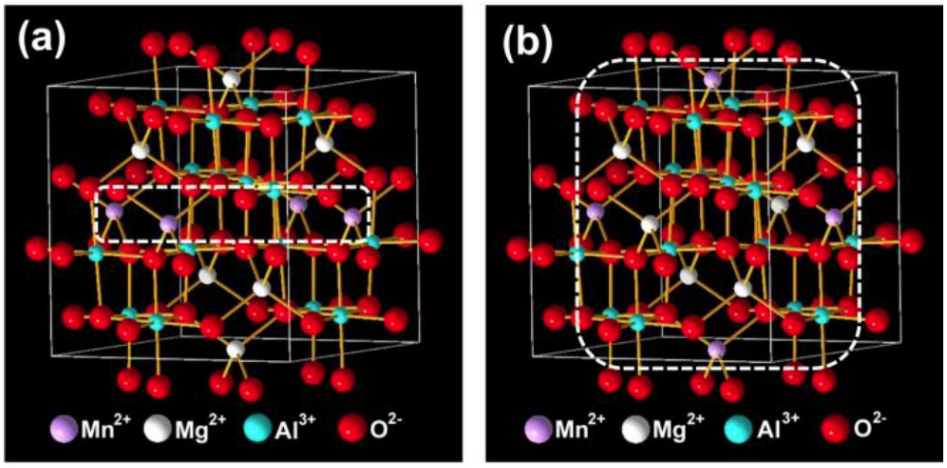

Scheme 1: Schematic illustration of the coordination model used for the (**a**) sample $MgAl_2O_4$:0.10%Mn^{2+} phosphor and the (**b**) reference product $MgAl_2O_4$:0.10%Mn^{2+} with 12wt% MgF_2 flux. The distribution of Mn^{2+} luminescent centers is indicated using white dotted boxes.

CONCLUSIONS

A traditional solid state method was used to prepare Mn^{2+} ions doped phosphors $MgAl_2O_4:Mn^{2+}$ [$n_{Mn}/(n_{Mn}+n_{Mg})$ = 0% ~ 0.50%)]. with and without MgF_2 flux. Due to charge-transfer deexcitation associated with the Mn^{2+} ion, the phosphor exhibits single red luminescence centred at 650 nm. The emission intensity of $MgAl_2O_4:Mn^{2+}$ increases firstly and then decreases with the Mn^{2+} concentration increasing, which is attributed to the concentration quenching effect. The optimal Mn doping content for the best luminescence is 0.10%. The fluorescence intensity of $MgAl_2O_4$:0.10%Mn^{2+} improves when added different contents of MgF_2 flux (1 wt% ~ 18 wt%). The enhanced performance in photoluminescence is attributed to both the high crystallinity and regular particle size by the addition of MgF_2 flux.

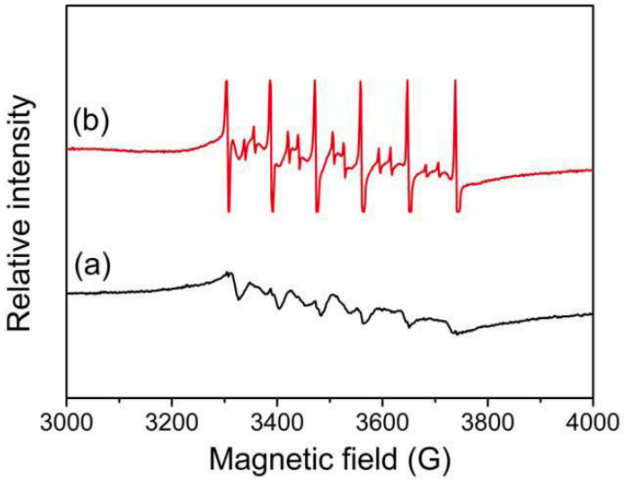

Figure 8: EPR spectra of the samples (a) $MgAl_2O_4$: 0.10%Mn^{2+}, (b) $MgAl_2O_4$:0.10% Mn^{2+} with 12 wt% MgF_2 flux.

ACKNOWLEDGEMENTS

This work was financially supported by the National Basic Research Program of China (2013CB934102), National Natural Science Foundation of China (21671134, 21331004, 21673140).

REFERENCES

[1] Schubert EF, Kim JK. Solid-State Light Sources Getting Smart. Science 2005; 308(5726): 1274-8. https://doi.org/10.1126/science.1108712

[2] Li YQ, Delsing ACA, de With G, Hintzen HT. Luminescence Properties of Eu^{2+} -Activated Alkaline-Earth Silicon-Oxynitride MSi_2 $O_{2-\delta}$ $N_{2+2/3\ \delta}$ (M = Ca, Sr, Ba): A Promising Class of Novel LED Conversion Phosphors. Chem Mater 2005; 17(12): 3242-8. https://doi.org/10.1021/cm050175d

[3] Dai Q, Foley ME, Breshike CJ, Lita A, Strouse GF. Ligand-Passivated Eu: Y_2O_3 Nanocrystals as a Phosphor for White Light Emitting Diodes. J Am Chem Soc 2011; 133(39): 15475-86. https://doi.org/10.1021/ja2039419

[4] Wang M-S, Guo S-P, Li Y, Cai L-Z, Zou J-P, Xu G, *et al.* A Direct White-Light-Emitting Metal−Organic Framework with Tunable Yellow-to-White Photoluminescence by Variation of Excitation Light. J Am Chem Soc 2009; 131(38): 13572-3. https://doi.org/10.1021/ja903947b

[5] Guo N, Song Y, You H, Jia G, Yang M, Liu K, *et al.* Optical Properties and Energy Transfer of NaCaPO4: Ce3+,Tb3+ Phosphors for Potential Application in Light-Emitting Diodes. Eur J Inorg Chem 2010; 2010(29): 4636-42. https://doi.org/10.1002/ejic.201000392

[6] Chiu C-H, Liu C-H, Huang S-B, Chen T-M. White-Light-Emitting Diodes Using Red-Emitting LiEu(WO[sub 4])[sub 2−x](MoO[sub 4])[sub x] Phosphors. J Electrochem Soc 2007; 154(7): J181. https://doi.org/10.1149/1.2731042

[7] Muthu S, Schuurmans FJP, Pashley MD. Red, green, and blue LEDs for white light illumination. IEEE J Sel Top Quantum Electron 2002; 8(2): 333-8. https://doi.org/10.1109/2944.999188

[8] Bachmann V, Ronda C, Meijerink A. Temperature Quenching of Yellow Ce $^{3+}$ Luminescence in YAG: Ce. Chem Mater 2009; 21(10): 2077-84. https://doi.org/10.1021/cm8030768

[9] Hou J, Yin X, Fang Y, Huang F, Jiang W. Novel red-emitting perovskite-type phosphor CaLa1−xMgM′O6: xEu3+ (M′ = Nb, Ta) for white LED application. Opt Mater 2012; 34(8): 1394-7. https://doi.org/10.1016/j.optmat.2012.02.031

[10] Piao X, Machida K, Horikawa T, Hanzawa H, Shimomura Y, Kijima N. Preparation of CaAlSiN $_3$: Eu $^{2+}$ Phosphors by the Self-Propagating High-Temperature Synthesis and Their Luminescent Properties. Chem Mater 2007; 19(18): 4592-9. https://doi.org/10.1021/cm070623c

[11] Nyman M, Shea-Rohwer LE, Martin JE, Provencio P. Nano-YAG: Ce Mechanisms of Growth and Epoxy-Encapsulation. Chem Mater 2009; 21(8): 1536-42. https://doi.org/10.1021/cm803137h

[12] Takahashi T, Adachi S. Mn4 + -Activated Red Photoluminescence in K2SiF6 Phosphor. J Electrochem Soc 2008; 155(12): E183-8.

[13] Adachi S, Takahashi T. Direct synthesis and properties of K2SiF6: Mn4+ phosphor by wet chemical etching of Si wafer. J Appl Phys 2008; 104(2): 023512. https://doi.org/10.1063/1.2956330

[14] Adachi S, Takahashi T. Photoluminescent properties of K2GeF6: Mn4+ red phosphor synthesized from aqueous HF/KMnO4 solution. J Appl Phys 2009; 106(1): 013516. https://doi.org/10.1063/1.3160303

[15] Adachi S, Takahashi T. Direct Synthesis of K2SiF6 : Mn4 + Red Phosphor from Crushed Quartz Schist by Wet Chemical Etching. Electrochem Solid-State Lett 2009; 12(2): J20-3.

[16] Arai Y, Adachi S. Optical properties of Mn4+-activated Na2SnF6 and Cs2SnF6 red phosphors. J Lumin 2011; 131(12): 2652-60. https://doi.org/10.1016/j.jlumin.2011.06.042

[17] Xu YK, Adachi S. Properties of Na2SiF6: Mn4+ and Na2GeF6: Mn4+ red phosphors synthesized by wet chemical etching. J Appl Phys 2009; 105(1): 013525. https://doi.org/10.1063/1.3056375

[18] Murata T, Tanoue T, Iwasaki M, Morinaga K, Hase T. Fluorescence properties of Mn4+ in CaAl12O19 compounds as red-emitting phosphor for white LED. J Lumin 2005; 114(3-4): 207-12. https://doi.org/10.1016/j.jlumin.2005.01.003

[19] Singh V, Natarajan V, Zhu J-J. Luminescence and EPR investigations of Mn activated calcium aluminate prepared via combustion method. Opt Mater 2007; 30(3): 468-72. https://doi.org/10.1016/j.optmat.2007.01.003

[20] Ye T, Li S, Wu X, Xu M, Wei X, Wang K, *et al.* Sol-gel preparation of efficient red phosphor Mg 2 TiO 4 : Mn 4+ and XAFS investigation on the substitution of Mn 4+ for Ti 4+. J Mater Chem C 2013; 1(28): 4327-33. https://doi.org/10.1039/c3tc30553h

[21] Ye R, Jia G, Deng D, Hua Y, Cui Z, Zhao S, *et al.* Controllable Synthesis and Tunable Colors of α- and β-Zn $_2$ SiO $_4$: Mn $^{2+}$ Nanocrystals for UV and Blue Chip Excited White LEDs. J Phys Chem C 2011; 115(21): 10851-8. https://doi.org/10.1021/jp2023633

[22] Tomita A, Sato T, Tanaka K, Kawabe Y, Shirai M, Tanaka K, *et al.* Luminescence channels of manganese-doped spinel. J Lumin 2004; 109(1): 19-24. https://doi.org/10.1016/j.jlumin.2003.12.049

[23] Song Y, Guo N, You H. Synthesis and Luminescent Properties of Cerium-, Terbium-, or Dysprosium-Doped Gd4Si2O7N2 Materials. Eur J Inorg Chem 2011; 2011(14): 2327-32. https://doi.org/10.1002/ejic.201001150

[24] Yang Z, Yang G, Wang S, Tian J, Li X, Guo Q, *et al.* A novel green-emitting phosphor NaCaPO4: Eu2+ for white LEDs. Mater Lett 2008; 62(12-13): 1884-6. https://doi.org/10.1016/j.matlet.2007.10.030

[25] Park YJ, Kim YJ. Blue emission properties of Eu-doped CaAl2O4 phosphors synthesized by a flux method. Mater Sci Eng B 2008; 146(1-3): 84-8. https://doi.org/10.1016/j.mseb.2007.07.048

[26] Wang Y, Wang Z. Characterization of Y2O2S: Eu3+, Mg2+, Ti4+ Long-Lasting Phosphor Synthesized by Flux Method. J Rare Earths 2006; 24(1): 25-8. https://doi.org/10.1016/S1002-0721(06)60059-8

[27] Zhang S, Zhuang W, Zhao C, He H, HUANG X. Influence of flux on properties of Y3Al5O12: Ce phosphor. J Chin Rare Earth Soc 2002; (06): 605-7.

[28] Ma, L, Hu, J. G., Wan, G. J., Hu, X. F., Yan, S. R., Yu, L. G. Effect of flux on YAG: Ce phosphors prepared by solid-state reactions. Chin J Lumin 2006; 27(3): 348-52.

[29] Nag A, Kutty TRN. Role of B2O3 on the phase stability and long phosphorescence of SrAl2O4: Eu, Dy. J Alloys Compd 2003; 354(1-2): 221-31. https://doi.org/10.1016/S0925-8388(03)00009-4

[30] Kottaisamy M, Jagannathan R, Rao RP, Avudaithai M, Srinivasan LK, Sundaram V. On the Formation of Flux Grown Y 2 O 2 S : Eu3 + Red Phosphor. J Electrochem Soc 1995; 142(9): 3205-9. https://doi.org/10.1149/1.2048714

[31] Lee HJ, Kim KP, Hong GY, Yoo JS. The effect of flux materials on the physical and optical properties of Eu3+-activated yttrium oxide phosphors. J Lumin 2010 Jun; 130(6): 941-6. https://doi.org/10.1016/j.jlumin.2010.01.002

[32] Feng Z, Zhuang W, Huang X, Wen X, Hu Y. Effect of MgF2-H3BO3 flux on the properties of (Ce,Tb)MgAl11O19 phosphor. J Rare Earths 2010; 28(3): 351-5. https://doi.org/10.1016/S1002-0721(09)60110-1

[33] Won HI, Nersisyan HH, Won CW, Lee KH. Effect of metal halide fluxes on the microstructure and luminescence of Y3Al5O12: Ce3+ phosphors. Mater Chem Phys 2011; 129(3): 955-60. https://doi.org/10.1016/j.matchemphys.2011.05.025

[34] Akselrud LG, Zavalii PY, Grin YN, Pecharski VK, Baumgartner B, Wölfel E. Use of the CSD Program Package for Structure Determination from Powder Data. Mater Sci Forum 1993; 133-136: 335-42. https://doi.org/10.4028/www.scientific.net/MSF.133-136.335

[35] Guo Y, Cao X, Lan X, Zhao C, Xue X, Song Y. Solution-Based Doping of Manganese into Colloidal ZnO Nanorods. J Phys Chem C 2008; 112(24): 8832-8. https://doi.org/10.1021/jp800106v

[36] Al P. Mechanism of concentration quenching of a xanthene dye encapsulated in phospholipid vesicles. Photochem Photobiol 1986; 44(4): 453-9. https://doi.org/10.1111/j.1751-1097.1986.tb04692.x

[37] Singh V, Chakradhar RPS, Rao JL, Kim D-K. Synthesis, characterization, photoluminescence and EPR investigations of Mn doped MgAl2O4 phosphors. J Solid State Chem 2007; 180(7): 2067-74. https://doi.org/10.1016/j.jssc.2007.04.030

[38] Zhong R, Zhang J, Wei H, Qi X, Li M, Han X. The different luminescent characteristics of MgAl2O4: Mn2+ between phosphor powder and nanoparticles. Chem Phys Lett 2011; 508(4-6): 207-9. https://doi.org/10.1016/j.cplett.2011.04.033

[39] Dai P, Zhang X, Sun P, Yang J, Wang L, Yan S, *et al.* Influence of Flux on Morphology and Luminescence Properties of Phosphors: A Case Study on Y1.55Ti2O7: 0.45Eu3+. Ballato J, editor. J Am Ceram Soc 2012; 95(4): 1447-53. https://doi.org/10.1111/j.1551-2916.2012.05092.x

[40] Shionoya, Shigeo, William M. Yen, Hajime Yamamoto. In: Phosphor Handbook. CRC press; 2006.

[41] Chang Y-S, Huang F-M, Chen H-L, Tsai Y-Y. Effects of Na2CO3 flux addition on the structure and photoluminescence properties for Eu3+-doped YVO4 phosphor. J Phys Chem Solids 2011; 72(10): 1117-21. https://doi.org/10.1016/j.jpcs.2011.06.008

[42] Su Y-K, Peng Y-M, Yang R-Y, Chen J-L. Effects of NaCl flux on microstructure and luminescent characteristics of KSrPO4: Eu2+ phosphors. Opt Mater 2012; 34(9): 1598-602. https://doi.org/10.1016/j.optmat.2012.03.019

Received on 29-05-2017 Accepted on 05-06-2017 Published on 23-10-2017

DOI: https://doi.org/10.12974/2311-8717.2017.05.01.3